Centennial glacier retreat as categorical evidence of regional climate change: supplementary information

Gerard H. Roe
Dept. Earth and Space Sciences, University of Washington, Seattle, WA.
gerard@ess.washington.edu

Marcia B. Baker
Dept. Earth and Space Sciences, University of Washington, Seattle, WA.
mbbaker@ess.washington.edu.

Florian Herla
Institute of Atmospheric and Croyspheric Sciences, University of Innsbruck, Austria
Florian.Herla@student.uibk.ac.at.

1 Similar results from alternative glacier models

In this section we demonstrate that an alternative glacier model gives similar answers to the three-stage model[S1] used in the main analysis. The three-stage model provides enhanced performance at high frequencies (i.e., $f > 1/(2\pi\tau)$) compared to an earlier class of analytic models that used a simple relaxation model of glacier dynamics (a *one-stage* model), represented by a first-order differential equation[S2,S3].

$$\left(\frac{d}{dt} + \frac{1}{\tau}\right) L' = \beta b'(t), \tag{S1}$$

Eq. (S1), and closely related equivalents, have been widely used in studies exploring glacier response to climate change[S4,S5,S6]. As such it is worth showing that, within our framework, one could use either Eq. (3) or Eq. (S1) and obtain similar results. For this one-stage model the equivalent solutions to Eq. (5) and (7) are:

$$\phi_1(t_o, \tau) = \tau \cdot \left[1 - \frac{\tau}{t_o}(1 - e^{-t_o/\tau})\right], \tag{S2}$$

and

$$\psi_1(\tau) = \tau \cdot \sqrt{\frac{\Delta t}{2\tau}}. \tag{S3}$$

and so the equivalent amplification factor for the one-stage model is given by $\gamma_1(t_o, \tau) = \phi_1(t_o, \tau)/\psi_1(\tau)$. Figure S1 compares the γs from the one-stage and three-stage equations and demonstrates that, for both models, $\gamma \sim 5$ to 6 in the parameter space applicable to alpine glaciers and century-scale climate trends. The value of γ for the one-stage model is slightly higher than for the three-stage model because, for a given τ, the one-stage equations respond more quickly to a trend. However, the essential point is that the detailed dynamics do not matter much - physical systems with decadal response times will act as sensitive amplifiers of centennial-scale climate change. We note

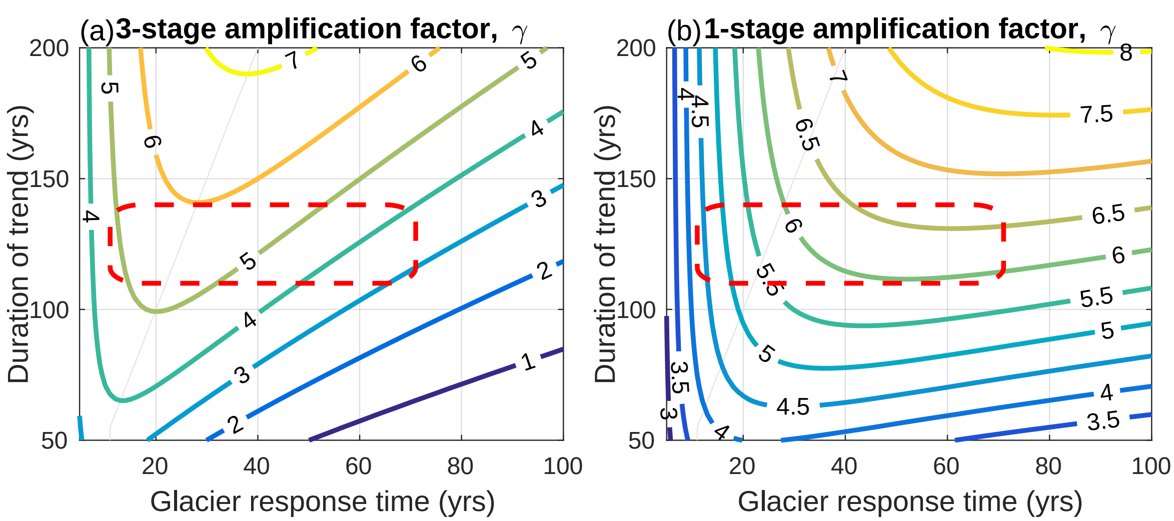

Figure S1: Amplification factor γ in the relationship $s_L = \gamma \cdot s_b$, contoured as a function of the glacier response time and the duration of the applied trend. (a) γ for the 3-stage model (Eq. 8), reproducing Figure 2b; (b) γ for the 1-stage model (Eq. S1). The red-dashed box shows the range of parameter space that applies for typical alpine glaciers and centennial-scale climate trends from anthropogenic climate change.

that ref. S3 uses an equation identical in form to Eq. (S1), but proposes a different, semi-empirical scaling for response time, $\tau \sim \bar{L}/u$, where $\bar{L}$ is the mean-state length and u is a characteristic velocity. Whereas ref. S7 took u to be the speed of kinematic surface waves at the terminus, ref. S3 relates u to mass flux and, via a scale analysis, to simple functions of glacier geometry, then finally calibrating it to the output of numerical models. Ref. S1 demonstrates that the original scaling of ref. S2 ($\tau = -H/b_t$) better captures glacier dynamics. But regardless, since there is uncertainty in H we include a broad uncertainty in our estimates of τ. In the next sections we derive two independent ways to estimate the signal-to-noise ratio of glacier length.

2 The PDF of the null hypothesis in the presence of climatic persistence

As noted in the main text and methods, we evaluated our modeled mass-balance time series, $b'(t)$, for the presence of persistence (i.e., autocorrelations in time, after linear detrending). 34 of the 37 mass-balance time series were consistent with white noise. However studies have shown that if persistence were present, it would enhance σ_L[S8,S9]. Various statistical models exist for representing such persistence. Ref. S9 showed that so-called 'power-law' persistence of the form $P(f) = P_0(f/f_0)^{-\eta}$, where $P(f)$ is the spectral power as a function of frequency f, had the largest impact on σ_L. Taking Hintereisferner again as an example, we find the power spectrum of the detrended $b'(t)$ is characterized by $\eta = 0.15 \pm 0.2$ (95% bounds), which is not statistically significant and thus consistent with the autoregression tests. Nevertheless we can take a what-if approach: in the event such persistence were present, what would the be impact on our conclusions? Following ref. S9 we generate long synthetic mass-balance times series in which power-law persistence is present (but with no underlying climate trend), and determine the null probability distribution of the ΔLs that arise in arbitrary 130 yr time periods as a result of this random climate variability. Fig. S2 shows the resulting PDFs for the parameters appropriate for Hintereisferner. Adding persistence does

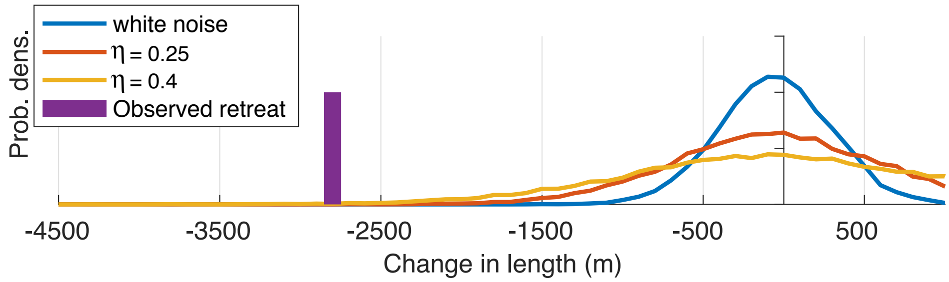

Figure S2: The impact of persistence on the null probability distribution of ΔL for Hintereisferner. The curves show the PDFs of ΔLs that occur for arbitrary 130-yr segments of long synthetic climate time series in which varying amounts of persistence of the form $P(f) = P_0(f/f_0)^{-\eta}$ have been added, but with no trend; and compared to the observed retreat of Hintereisferner. PDF areas are normalized to 1.

broaden the distribution of $\Delta L|^{null}$. However, even for the extreme case of $\eta = 0.4$, the probability of the observed glacier retreat remains less than 1%. Thus our conclusion that it is '*virtually certain*' the observed retreat required a climate change remains the same.

3 Application to a global distribution of glaciers

We apply our analysis to 37 glaciers across five geographic regions (the Alps, Scandinavia, North America, Asia, the Southern Hemisphere). Data for glacier length comes from ref. S6; and for mass balance from the World Glacier Monitoring Service (WGMS)[S10], unless otherwise noted in the SI spreadsheet. The two other key factors are b_t, the annual mass balance at the terminus, and H the characteristic thickness near the terminus. We draw on a variety of sources for these, but primarily b_t is taken from vertical mass-balance profiles reported by WGMS; where possible H is taken from observed or modeled glacier profiles, otherwise we use the thickness scalings provided by ref. S11 and S12, from which H can be estimated from other geometric glaciers parameters provided by the WGMS[S10].

In the supplementary spreadsheet, the complete set of parameters for all 37 glacier are provided, along with their sources (refs. S10 to S43). We preferentially selected valley glaciers with long mass-balance records (or long records from nearby glaciers), and continuous length histories without long gaps. We could not always satisfy these conditions, particularly for glaciers in Asia and South America, which typically have sparse length histories. For 16 of the 37 glaciers the length records are too sparse to determine the degrees of freedom (these glaciers are indicated in SI spreadsheet), and for these we stipulate a flat, negative definite prior on s_L. This choice for $h_{s_L}|^{L_{obs}}$ is consistent with the observed retreat ($\Delta L < 0$) of all these glaciers (Figs. 1 and S3 to S7); and also with the modeled negative mass balance (due primarily to the observed warming trends, all of which are significant at the 5% level). Characteristic glacier response times of several decades mean we can be certain that, despite only having sparse observations, we have not mistakenly identified as a retreat what was actually an overall advance. In many instances this can be verified by evidence that is additional to the formal length measurements including aerial photography, historical records, and geomorphic analysis. Given $\Delta L < 0$, and since σ_L is positive definite, $s_L|^{obs}$ must be negative. Further, this flat PDF allows the possibility that s_L is arbitrarily close to zero, which implies arbitrarily large σ_L. When combined with our climate-based PDF, $h_{s_L}(s_L)|^{T,P_{obs}}$, our analyses for several glaciers do indeed show upper bounds (97.5%) of $\sigma_L \gg 1$ km (Fig. 1, S3 to S7, and SI spreadsheet). The potential for such large σ_L acts to increase p_L^{null} (the probability the observed retreat could have happened in a constant climate). However, it is likely that such large values for σ_L can be ruled out on physical grounds, particularly for arid climates and smaller glaciers. Although not part of our analyses here, analytical (i.e., Eq. 6) or numerical modeling that included parameter uncertainty would help constrain σ_L, and would very likely further decrease p_L^{null} in these cases.

For completeness, for all glaciers we report the statistical significance evaluated using both the full analyses (i.e., combining $h_{s_L}|^{L_{obs}}$ and $h_{s_L}|^{T,P_{obs}}$ using Bayes' theorem), and also stipulating a flat, negative-definite prior for $h_{s_L}|^{L_{obs}}$ instead. Finally, for clarity, we also present the results of the analysis graphically for all five regions (Figs. S3 to S8).

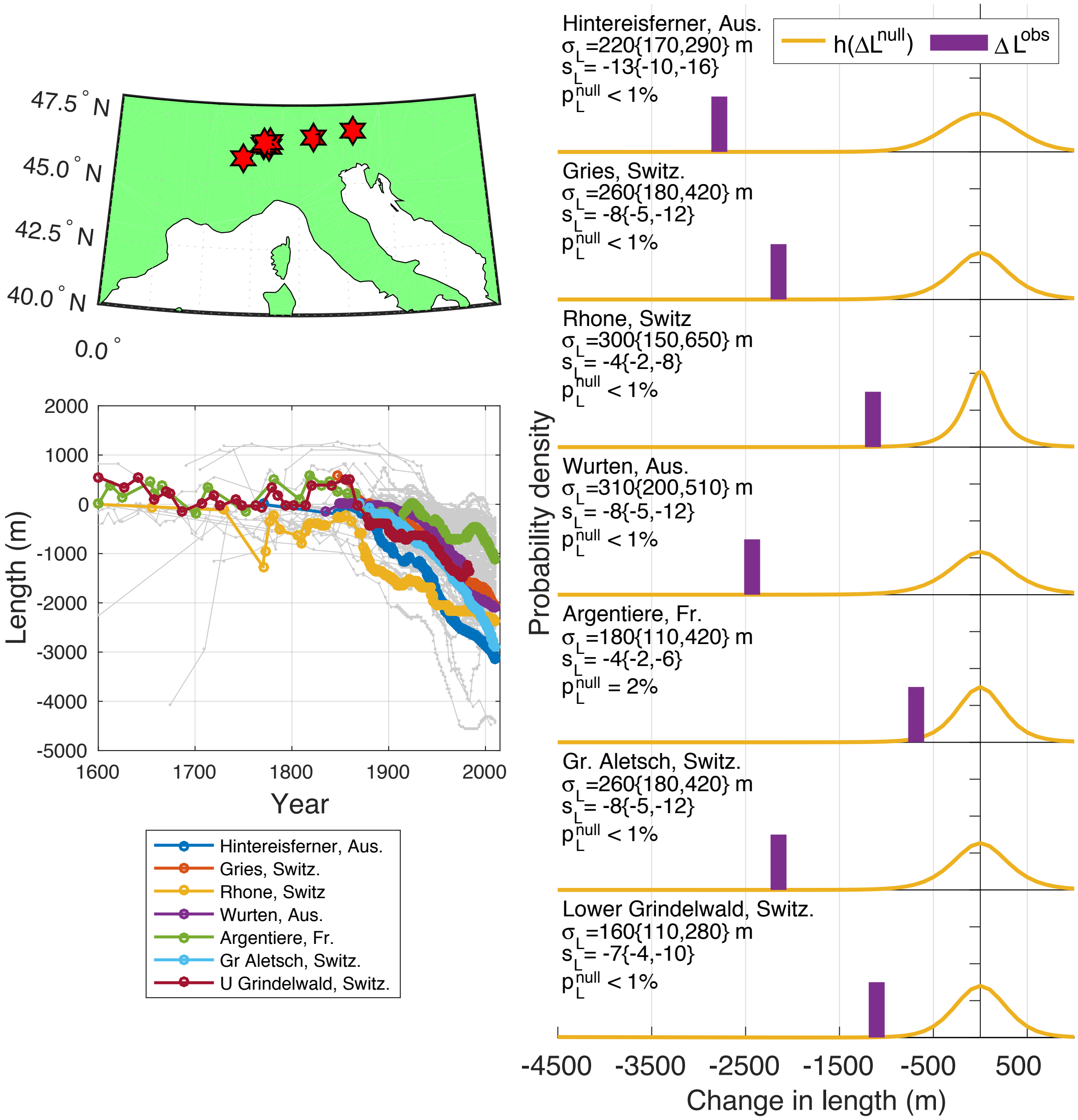

Figure S3: Glacier analyses in the European Alps. The top left panel show the locations of the glacier analyzed. The bottom left panel shows the length histories and length histories of the glaciers analyzed. Right panels are as for Fig. 4.

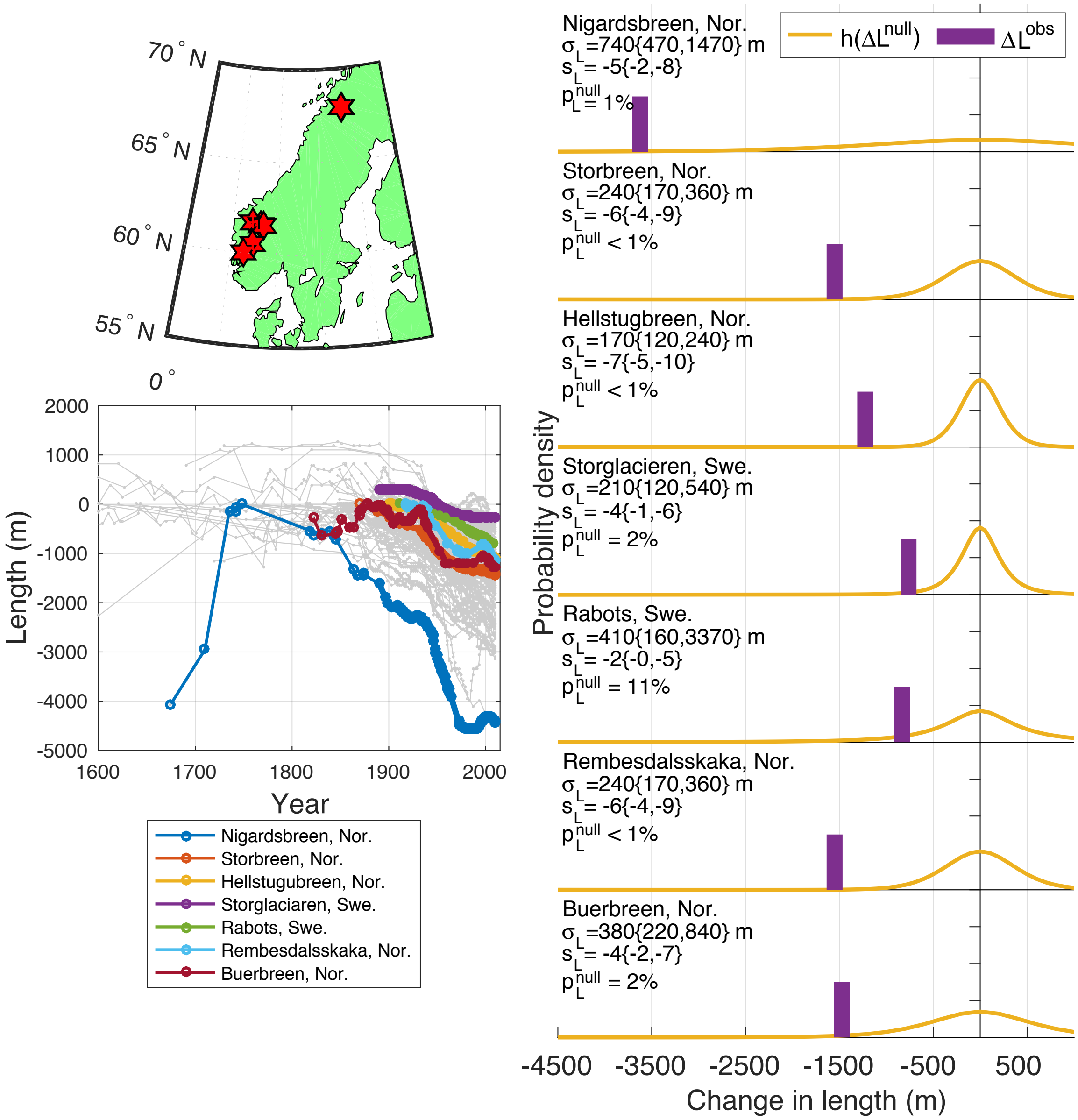

Figure S4: As for Fig. S3, but for analyzed glaciers in Scandinavia.

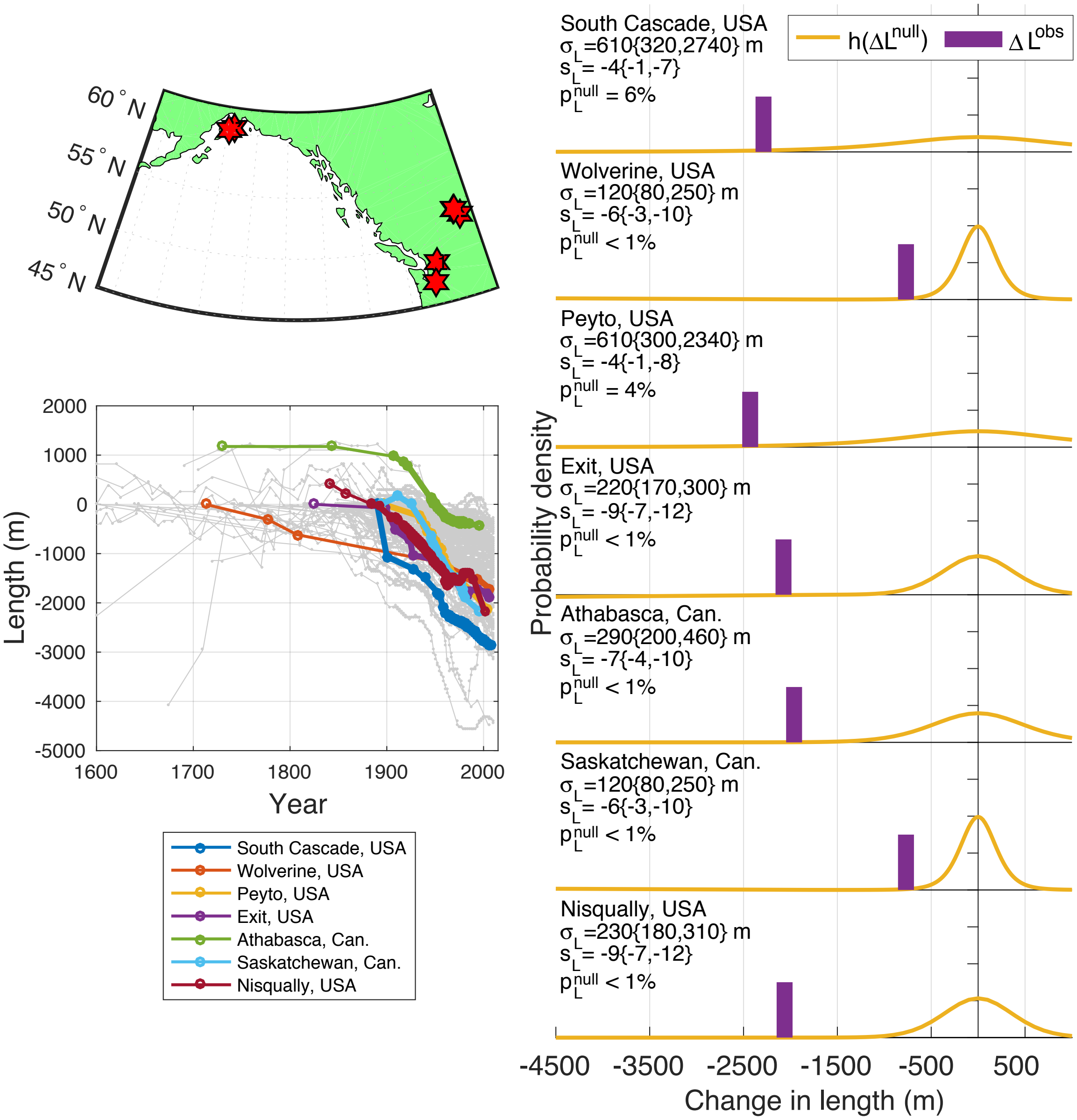

Figure S5: As for Fig. S3, but for analyzed glaciers in North America.

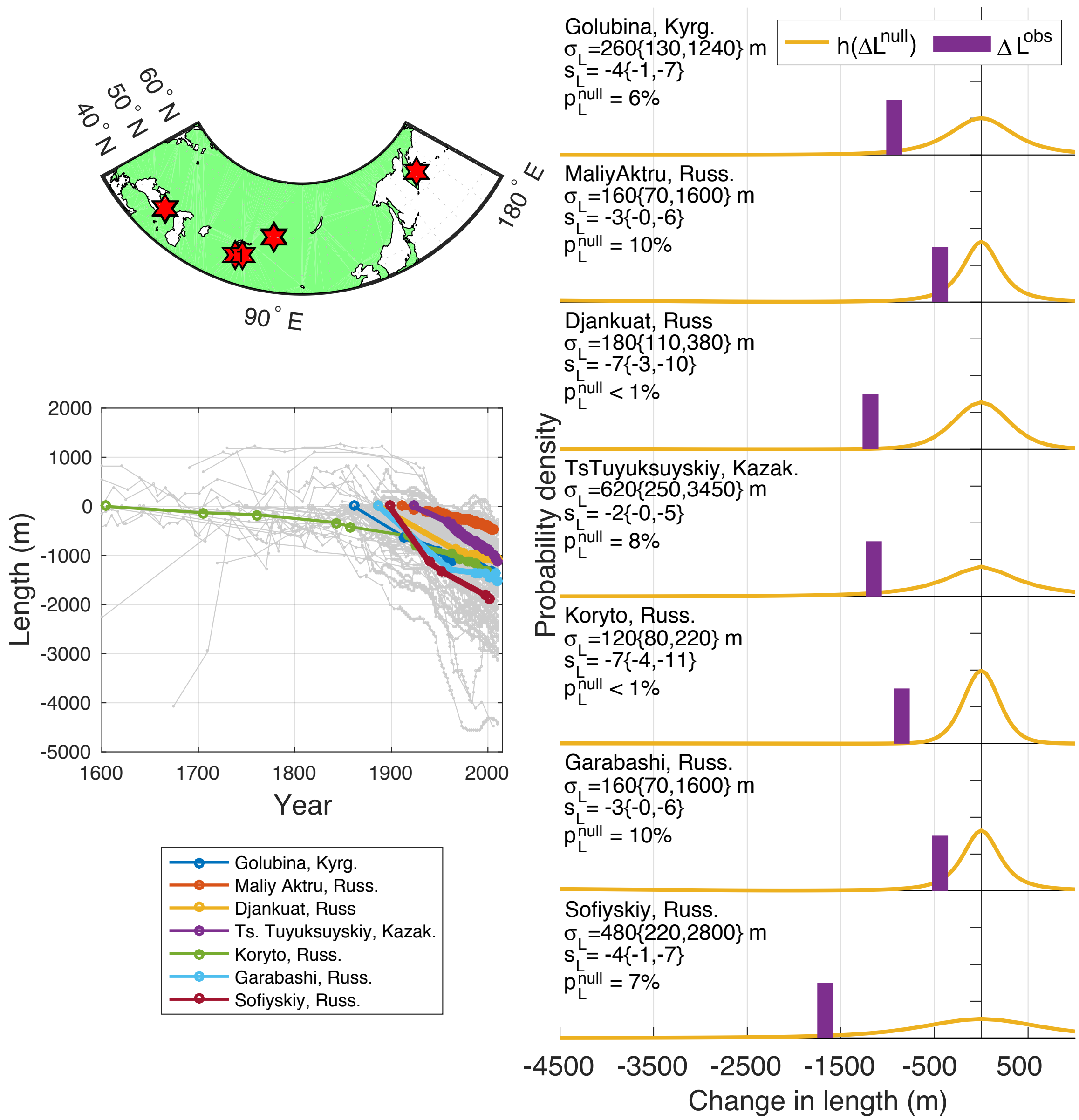

Figure S6: As for Fig. S3, but for analyzed glaciers in Asia.

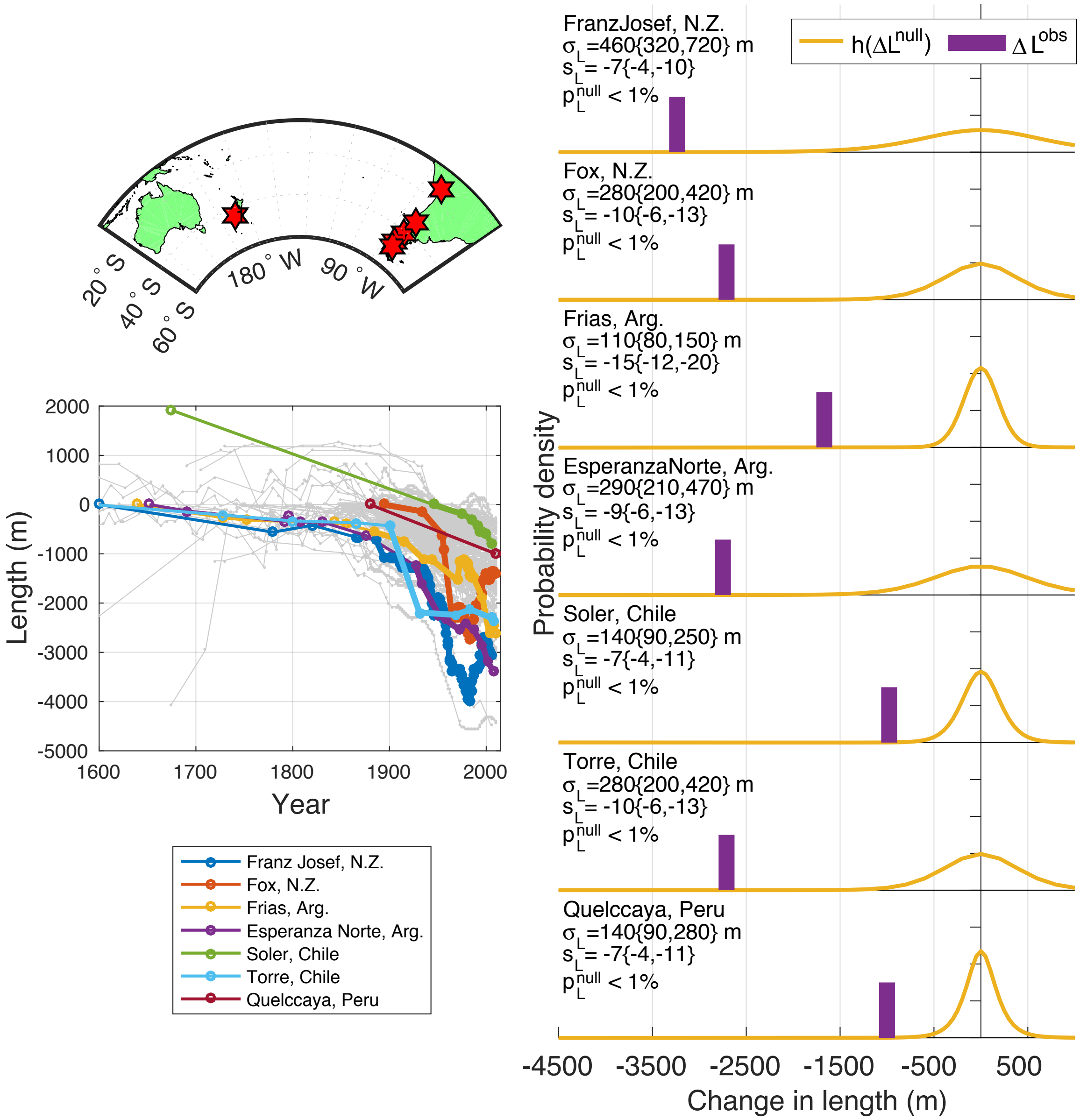

Figure S7: As for Fig. S3, but for analyzed glaciers in the Southern Hemisphere.

References:

S1. Roe., G.H. & Baker, M. B. Glacier response to climate perturbations: an accurate linear geometric model. *J. Glaciol.* **60**, 670-684 (2014).

S2. Jóhannesson, T., Raymond, C. F. & Waddington, E. D. Timescale for adjustments of glaciers to changes in mass balance. *J. Glaciol.* **35**, 355-369 (1989).

S3. Oerlemans, J., *Glaciers and climate change*. Lisse, etc., A.A. Balkema (2001).

S4. Oerlemans, J. Extracting a climate signal from 169 glacier records. *Science* **308**, 675-677 (2005).

S5. Raper, S. C. B. & Braithwaite, R. J. Glacier volume response time and its links to climate and topography based on a conceptual model of glacier hypsometry. *The Cryosphere* **3**, 183-194 (2009).

S6. Leclercq, P.W. & Oerlemans, J. Global and hemispheric temperature reconstruction from 491 glacier length fluctuations. *Clim. Dyn.* **38**, 1065-1079 (2011).

S7. Nye, J .F. The response of glaciers and ice sheets to seasonal and climatic changes. *Proc. R. Soc. London. Ser. A* **256**, 559-584 (1960).

S8. Reichert, B.K., Bengtsson, L. & Oerlemans, J. Recent glacier retreat exceeds internal variability. *J. Climate* **15**, 3069-3081 (2002).

S9. Roe, G.H. & and Baker, M.B. The response of glaciers to climatic persistence. *J. Glaciology* DOI: 10.1017/jog.2016.4 (2016)

S10. WGMS. *Fluctuations of Glaciers Database.* World Glacier Monitoring Service, Zurich, Switzerland. DOI:10.5904/wgms-fog-2014-09. Online access: http://dx.doi.org/10.5904/wgms-fog-

2014-09 (2014).

S11. Haeberli, W. & Hoelzle, M. Application of inventory data for estimating characteristics of and regional climate-change effects on mountain glaciers: a pilot study with the European Alps. *Ann. Glaciol.* **21**, 206-212 (1995).

S12. Hoelzle, M., Chinn, T., Stumm, D., Paul, F., Zemp, M. & Haeberli W. The application of glacier inventory data for estimating past climate change effects on mountain glaciers: A comparison between the European Alps and the Southern Alps of New Zealand. *Glob. and Plan. Change* **56(12)**, 69-82 (2007).

S13. Greuell, W. Hintereisferner, Austria: mass-balance reconstruction and numerical modelling of the historical length variations. *J. Glaciology* **38**, 233-244 (1992).

S14. Schlosser, E., Numerical simulation of fluctuations of Hintereisferner, Ötztal Alps, since ad 1850. *Ann. Glaciol.* **24**, 199-202 (1996).

S15. Schwitter, M.P. & Raymond, C. F. Changes in the longitudinal profiles of glaciers during advance and retreat. *J. Glaciol.* **39(133)**, 582-590 (1993).

S16. Woo, M. & Fitzharris B. B. Reconstruction of mass-balance variations for Franz Josef Glacier, New Zealand. *Arct. Alp. Res.* **24**, 281-290 (1992).

S17. Anderson, B., Lawson, W., & Owens, I. Response of Franz Josef Glacier *Ka Roimata o Hine Hukatere* to climate change. *Glob. Plan. Change* **63**, 23-30 (2008).

S18. Oerlemans, J. Climate sensitivity of Franz Josef Glacier, New Zealand, as revealed by numerical modelling. Arctic and Alpine Research **29**, 233-239 (1997).

S19. Leclercq, P. W., Pitte, P., Giesen, R. H., Masiokas, M. H. & Oerlemans, J. Modelling and climatic interpretation of the length fluctuations of Glaciar Frías (north Patagonian Andes, Argentina) 1639-2009 AD. *Climate of the Past* **8**, 1385-1402, doi: 10.5194/cp-8-1385-2012 (2012).

S20. Van Beusekom, A. E., ONeel, S. R., March, R. S., Sass, L. C. &Cox, L. H. Re-analysis of alaskan benchmark glacier mass-balance data using the index method. *US Geological Survey Scientific Investigations Report* **5247**, 16 (2010).

S21. Clarke, G. K. C., Anslow, F. S., Jarosch, A. H., Radic, V., Menounos, B., Bolch, T. & Berthier, E. Ice volume and subglacial topography for western Canadian glaciers from mass balance fields, thinning rates, and a bed stress model. *J. Climate* **26**, 4282-4303. doi:10.?1175/?JCLI-D-12-00513.?1 (2013).

S22. Meier, M. F. & Post, A. Recent variations in mass net budgets of glaciers western North America. *IUGG/IAHS Pub.* **58**, 63-77 (1962).

S23. Meier, M.F., Rigsby, G. P. & Sharp, R. P. Preliminary data from Saskatchewan Glacier, Alberta, Canada. *Arctic* **7**, 3-26 (1954).

S24. Rasmussen, L.A. & Wenger, J. M. Upper-air model of summer balance on Mt. Rainier, USA. *J Glaciology* **55**, 619-624 (2009).

S25. Yamaguchi, S., Naruse, R. & Shiraiwa, T. Climate reconstruction since the Little Ice Age by modelling Koryto glacier, Kamchatka Peninsula, Russia. *J. Glaciology* **54(184)**, 125-130 (2008).

S26. Pattyn, F., De Smedt, B., De Brabander, S., Van Huele, W., Agatova, A., Mistrukov, A. & Decleir, H. Ice dynamics and basal properties of Sofiyskiy Glacier, Altai Mountains, Russia based on DGPS and radio-echo sounding surveys. *Ann. Glaciol.* **37**, 286-292 (2003).

S27. Cherkasov, P. A., Ahmetova, G. S., & Hastenrath, S. Ice flow and mass continuity of Shumsky Glacier in the Djungarski Alatau Range of Kazakhstan, Central Asia. *J. Geophys. Res.* **101**, 12,913-12,920 (1996).

S28. Grove J. M. *Little Ice Ages: Ancient and Modern. Second edition.* London and New York: Routledge, 2 vols (2004).

S29. Schaefer, M., Machguth, H., Falvey, M. and Casassa, G. Modeling past and future surface mass balance of the Northern Patagonia Icefield, *J. Geophys. Res. Earth Surf.*, **118**, 571-588, doi:10.1002/jgrf.20038 (2013).

S30. Popovnin, V. V., Danilova, T. A. & Petrakov, D. A. A pioneer mass balance estimate for a Patagonian glacier: Glaciar de los Tres, Argentina.]*Global and Planetary Change* **22**, 255-267 (1999).

S31. Kelly, M. A., Lowell, T. V., Applegate, P. J., Smith C. A., Phillips, F. M., & Hudson, A. M. Late glacial fluctuations of Quelccaya Ice Cap, southeastern Peru. *Geology* **40**, 991-994 (2012).

S32. Malone A. G. O., Pierrehumbert, R. T., Lowell, T. V., Kelly, M. A. & Stroup, J. S. Constraints on southern hemisphere tropical climate change during the Little Ice Age and Younger Dryas based on glacier modeling of the Quelccaya Ice Cap, Peru. *Quat. Sci. Rev.* **125**, 106-116 (2012).

S33. Purdie, H., Brook, M. & Fuller, I. Seasonal variation in ablation and surface velocity on a temperate maritime glacier: Fox Glacier, New Zealand. *Arct. Antarct. Alp. Res.* **40(1)**, 140-147 (2008).

S34. Chen, J. & Funk, M. Mass Balance of Rhonegletscher during 1882/83-1986/87. *J. Glaciology*

36(123) 199-209 (1990).

S35. Goehring, B. M., Vacco, D. A., Alley, R. B. & Schaefer, J. M. Holocene dynamics of the Rhone Glacier, Switzerland, deduced from ice flow models and cosmogenic nuclides. *Earth and Planetary Science Letters* **351-352**, 27-35 (2012).

S36. Jouvet, G., Huss, M., Funk, M. & Blatter, H. Modelling the retreat of Grosser Aletschgletscher, Switzerland, in a changing climate. J. Glac. **57(206)**, 1033-1046 (2011).

S37. Huss, M., Bauder, A., Funk M. & Hock, R. Determination of the seasonal mass balance of four Alpine glaciers since 1865. *J. Geophys. Res.* **113(F1)**, doi:10.1029/2007JF000803 (2008)

S38. Huybrechts, P., de Nooze, P. & Decleir, H. Numerical modelling of Glacier dArgentire and its historic front variations. In Oerlemans, J., editor, *Glacier fluctuations and climatic change*, Dordrecht: Kluwer Academic Publishers, 373-389 (1989).

S39. Schmeits, M. J. & Oerlemans, J. Simulation of the historical variation in length of the Unterer Grindelwaldgletscher, Switzerland. *J. Glac.* **43(143)**, 152-164 (1997).

S40. Andreassen, L. M., Huss, M., Melvold, K., Elvehøy, H. & Winsvold, S. H. Ice thickness measurements and volume estimates for glaciers in Norway. *J. Glac.* **61(228)**, 763-775 (2015).

S41. Stroeven, A. P. The robustness of one-dimensional, time-dependent, ice-flow models: A case study from Storglaciaren, northern Sweden. *Geogr. Ann.* **78 A (2-3)** 133-146 (1996).

S42. Björnsson, H. Radio-echo sounding maps of Storglaciären, Isfallsglaciären and Rabots glaciär, northern Sweden. *Geogr. Ann.* **63 A (3-4)** 225-231 (1981).

S43. Giesen, R. H. & J. Oerlemans, J. Response of the ice cap Hardangerjøkulen in southern Norway to the 20th and 21st century climates. *Cryosphere* **4(2)**, 191-213 (2010).